DYNLT3 Is Required for Chromosome Alignment During Mouse Oocyte Meiotic Maturation

Xin Huang, MS[1,2], Hai-Long Wang, PhD[1], Shu-Tao Qi, MS[2], Zhen-Bo Wang, PhD[2], Jing-Shan Tong, PhD[2], Qing-Hua Zhang, PhD[2], Ying-Chun Ouyang, PhD[2], Yi Hou, PhD[2], Heide Schatten, PhD[3], Zhong-Quan Qi, PhD[1], and Qing-Yuan Sun, PhD[2]

Abstract

Dynein light chain, Tctex-type 3 (DYNLT3), is a member of the cytoplasmic dynein DYNLT light chain family and has been reported to have a potential role in chromosome congression in human mitosis. However, its role in mammalian meiosis is unclear. In this study, we examined its localization, expression, and functions in mouse oocyte meiosis. Immunofluorescent staining showed that DYNLT3 was restricted to the germinal vesicle and associated with kinetochores at the germinal vesicle breakdown stage, metaphase I and metaphase II. The expression level of DYNLT3 was similar at all meiotic stages. Depletion of DYNLT3 by antibody injection resulted in chromosome misalignment and decrease of the polar body extrusion rate. We further found that DYNLT3-depleted oocytes displayed kinetochore-microtubule detachments. Chromosome-spread experiments showed that depletion of DYNLT3 inhibited the metaphase-anaphase transition by preventing homologous chromosome segregation in meiosis I. Our data suggest that DYNLT3 is required for chromosome alignment and homologous chromosome segregation during mouse oocyte meiosis.

Keywords

DYNLT3, mouse oocyte, kinetochore, microtubule, meiosis

Introduction

In mitotic and meiotic cells, accurate chromosome segregation ensures proper distribution of genetic material, while errors in this process will result in aneuploidy and developmental defects.[1,2] Kinetochores are chromosome-associated protein assemblies that form to mediate force interactions with microtubules, microtubule binding proteins, and additional components required for cell cycle regulation.[3] An intriguing component of the more elaborated outer kinetochore is the cytoplasmic microtubule motor dynein. During the G2/M transition, dynein becomes released from interphase cargos and localizes to three loci that are important for mitosis: (1) the cell cortex, (2) spindle poles, and (3) kinetochores.[3] The polar and cortical localizations of dynein reflect roles in spindle integrity and spindle positioning.[4-6] The kinetochore dynein has been implicated in microtubule attachment,[7,8] chromosome movement,[9] and regulation of the spindle assembly checkpoint (SAC).[10] Initial microtubule attachments to kinetochores is coupled to rapid poleward movement of the mono-oriented chromosomes.[9] More recent studies have found that dynein could be involved in reorienting tangential attachments to end-on attachment[11]; displacement of the motor domain of dynein from kinetochores destabilized kinetochores, suggesting a potential role for dynein in stabilizing kinetochores.[12]

Cytoplasmic dynein 1 is a microtubule minus end-directed motor protein responsible for multiple important mitotic and meiotic cellular processes. It is a multimeric complex composed of 2 dynein heavy chains, each containing motor domains that generate the force necessary to move along the microtubule.[13,14] In addition, the cargo binding domain of the complex consists of 5 subunits that assemble into the complex: the intermediate chain, light intermediate chain, and 6 light chains.[15-17] There are 3 different light chain families, DYNLL (previously called LC8), DYNRB (previously called roadblock), and DYNLT. DYNLT light chain plays important roles in multiple cellular events. The DYNLT light chain

[1] Organ Transplantation Institute, Xiamen University, Xiamen City, Fujian Province, China
[2] State Key Laboratory of Reproductive Biology, Institute of Zoology, Chinese Academy of Sciences, Beijing, China
[3] Department of Veterinary Pathobiology, University of Missouri, Columbia, MO, USA

Corresponding Author:
Zhong-Quan Qi, Organ Transplantation Institute, Xiamen University, 168 Daxue Road, Siming, Xiamen 361005, China.
Email: oti@xmu.edu.cn

family has 2 members, DYNLT1 (previously called Tctex1) and DYNLT3 (previously called Rp3).[18] DYNLT1 has been implicated in varied functions including non-Mendedilian meiotic drive,[19] production of functional sperm,[20] regular oscillatory nuclear movement in meiotic prophase in fission yeast,[21] and element direction that contributes to neural stem progenitor cells in brain.[22,23] Besides these functions, the target protein binding function of DYNLT1 has become a major research focus. DYNLT1 has been shown to bind many proteins, including Fyn,[24] DOC2,[25] CD5,[26] rhodopsin,[27] dynein intermediate chain,[28] Tastin,[29] CD155,[30] BMPR-II,[31] PTHR,[32] VP26[33] and Lfc,[34] and others. Another member of the DYNLT light chain family, DYNLT3 has been found to express in all cells and tissues so far[18,35]; it is also proposed to incorporate into dynein complexes responsible for binding dynein to specific cargoes. Dynein cargo binding function is temporally and spatially regulated and can be mediated by direct protein-protein interaction between cargo receptor and DYNLT light chains. For example, DYNLT1 and DYNLT3 competitively bind to dynein intermediate chain.[36,37] In addition, DYNLT3 has been shown to interact with VP26 and Bub3.[38-40] However, only Bub3 is the confirmed specific DYNLT3 interacting protein. Human DYNLT1 and DYNLT3 share 55% identity and they exhibit similar localization to microtubules at mitotic metaphase.[38,41] It is further known that both DYNLT1 and DYNLT3 may interact with other proteins to participate in assembly of microtubule in mitosis.[34,37,38,42]

All previous studies on DYNLT light chain have mainly been focused on its cargo binding function, but its role in mammalian meiosis remains unknown. Here, we show the localization and expression of DYNLT3 in mammalian oocyte meiotic maturation. We also explored its potential roles in chromosome alignment and maintenance of meiosis progression by protein depletion approach.

Materials and Methods

All chemicals and culture media were purchased from Sigma Chemical Company (St Louis, Missouri) unless stated otherwise.

Oocyte Collection and Culture

Care and handing of 4- to 6-week-old ICR mice were conducted in accordance with policies promulgated by the Ethics Committee of the Institute of Zoology, Chinese Academic of Sciences. Oocytes were cultured in M2 medium under paraffin oil at 37°C in a humidified atmosphere of 5% CO_2 in air. Oocytes were collected at different times of culture for immunostaining and Western blotting.

DYNLT3 Plasmid Construction and mRNA Synthesis

Total RNAs were extracted from 150 germinal vesicle (GV) stage mouse oocytes using RNeasy micro purification kit (Qiagen). By using cDNA synthesis kit (TaKaRa), we synthesized total cDNAs from the extracted total RNAs with poly (dT) as the primers. Then we cloned the full length DYNLT3 CDS by Nest PCR using 2 pairs of nest primers (Invitrogen). F1: 5′-GGA CTC AGA AAG CCA CCA- 3′, R1: 5′-AGA AAG GAT ACA CTC ACA AACT- 3′; F2: 5′-TCA GGC CGG CCG ATG GAG GGG TAC CAA CG- 3′, R2: 5′-GTT GGC GCG CCC TAC AGG ACA ATC GCA ACT- 3′. Next, the full DYNLT3 CDS was cloned to pCS2+ vector, which already had a Myc-tag behind the SP6 promoter for detection of the expressed protein. The Myc-DYNLT3-pCS2+ plasmid was linearized by endonucleases *SalI* and purified by gel extraction kit (Promega). SP6 high-yield capped RNA transcription kit (Ambion) was used for producing capped mRNA, and then the mRNA was purified with RNeasy cleanup kit (Qiagen). The concentration of DYNLT3 mRNA was detected with a Beckman DU 530 Analyzer, and then diluted to a low concentration (0.4 mg/mL) to localize the DYNLT3 protein.

Microinjection of Myc-DYNLT3 mRNA or DYNLT3 Antibody

About 5 to 10 pl low concentration DYNLT3 mRNA solution or mouse monoclonal anti-DYNLT3 antibody (Millipore) was microinjected into the cytoplasm of a fully grown GV oocyte using a Nikon Diaphot ECLIPSE TE300 (Nikon UK Ltd.) inverted microscope equipped with Narishige MM0-202N hydraulic 3-dimensional micromanipulators (Narishige Inc.). After microinjection, the oocytes were cultured in fresh M2 medium under paraffin oil at 37°C, in an atmosphere of 5% CO_2 in air. The control oocytes were microinjected with 5 to 10 pl Myc mRNA solution or rabbit immunoglobulin G (IgG) of the same concentration. Finally, after 8 and 12 hours of culture, oocyte phenotypes were examined by confocal microscopy.

Western Blot

Mouse oocytes were collected in SDS sample buffer and heated for 5 minutes at 100°C. The proteins were separated by SDS-PAGE and electrically transferred to polyvinylidene fluoride membrane, and then the membrane was blocked in TBST containing 5% skimmed milk for 2 hours, followed by incubation overnight at 4°C with mouse monoclonal anti-DYNLT3 antibody (1:250, Millipore) and rabbit monoclonal anti-β-actin antibody (1:1000, Zhong Shan Jin Qiao company). After washing 3 times in TBST each for 10 minutes, the membrane was incubated for 1 hour at 37°C with peroxidase-conjugated rabbit anti-mouse IgG (1:1000, Zhong Shan Jin Qiao Company) and peroxidase-conjugated mouse anti-rabbit IgG (1:1000, Zhong Shan Jin Qiao Company), respectively. Finally, the membrane was processed using the SuperSignal West Femto maximum sensitivity substrate (Thermo Scientific).

Chromosome Spread

Oocytes were left in hypotonic sodium citrate (1%, W/V) for 15 minutes at room temperature, and then placed on a glass slide. About 100 μL methanol: glacial acetic acid (3:1) was dropped onto the oocyte for fixation. Chromosomes were stained with PI (10 μg/mL). The specimen was examined with a Confocal Laser Scanning Microscope (Zeiss LSM 510 META, Germany).

Cold Treatment of Oocytes

DYNLT3 antibody and control IgG injected oocytes were cultured for 8 hours, and then transferred to M2 medium which was precooled to 4°C and cultured for 10 minutes. After treatment, oocytes were used for immunofluorescent experiments.

Immunofluorescent Staining

For single staining of Myc-DYNLT3 or α-tubulin, oocytes were fixed with 4% paraformaldehyde in PBS for 30 minutes at room temperature. Then they were transferred to membrane permeabilization solution (0.5% Triton X-100) for 20 minutes. After 1 hour block in blocking buffer (1% BSA-supplemented PBS), oocytes were incubated overnight at 4°C with FITC-anti-Myc antibody (1:100, Invitrogen) or anti-α-tubulin-FITC antibody (1:200) respectively. After 3 washes in washing buffer (0.1% Tween 20 and 0.01% Triton X-100 in PBS), the oocytes were stained with propidium iodide (PI, 10 μg/mL in PBS) for 15 minutes with 1 additional wash in washing buffer.

For double staining of Myc-DYNLT3 and CREST or α-tubulin and CREST, after staining of Myc-DYNLT3 or α-tubulin and 3 washes in washing buffer for 5 minutes each, oocytes were again blocked in blocking buffer for 1 hour at room temperature, then oocytes were stained with human anti-CREST antibody (1:50, Fitzgerald) overnight at 4°C. After 3 washes in washing buffer (0.1% Tween 20 and 0.01% Triton X-100 in PBS), the oocytes were labeled with CY5-conjugated goat anti-human IgG (1:100, Jackson ImmunoResearch) for 1 hour at room temperature. After the oocytes were further washed 3 times in washing buffer (0.1% Tween 20 and 0.01% Triton X-100 in PBS), they were stained with PI (10 μg/mL in PBS) for 15 minutes with 1 additional wash in washing buffer.

Finally, the oocytes were mounted on glass slides and examined with a Confocal Laser Scanning Microscope (Zeiss LSM 510 META, Germany).

Statistical Analysis

Data (mean $\pm$ SEM) were from at least 3 replicates per experiment and analyzed by analysis of variance (ANOVA) using SPSS software (SPSS Inc, Chicago, Illinois) followed by student-Newman-Keuls test. The number of oocytes was labeled in parentheses as (n). Difference at $P < .05$ was considered to be statistically significant and different superscripts indicate the statistical difference.

Results

Localization and Expression of DYNLT3 During Mouse Oocyte Meiotic Maturation

Due to the lack of availability of antibody for DYNLT3 immunofluorescent staining, we injected a low concentration of exogenous Myc-DYNLT3 mRNA (0.4 mg/mL, about 5 to 10 pl/oocyte) into GV stage oocytes to determine the subcellular distribution of DYNLT3 at different meiotic stages. As shown in Figure 1A, in the GV oocytes, DYNLT3 was mainly concentrated in the germinal vesicle. After germinal vesicle breakdown (GVBD), DYNLT3 accumulated at the kinetochores. By metaphase I (MI) and metaphase II (MII), DYNLT3 was still located at the kinetochores. Colocalization of Myc-DYNLT3 with CREST (a marker of CENPs at the kinetochores) confirmed the kinetochore distribution pattern of DYNLT3 (Figure 1C).

We cultured oocytes for 0, 4, 8, 9.5, and 12 hours, the time points when most oocytes reached GV, prometaphase I (Pro MI), MI, anaphase-telophase I (ATI), and MII stages, respectively, to examine the expression of DYNLT3 during mouse oocyte meiotic maturation. The immunoblotting results (Figure 1B) showed that the DYNLT3 expression level was similar at all meiotic stages.

Depletion of DYNLT3 Affected Chromosome Alignment and Disrupted the Attachment Between Microtubules and Chromosomes

To investigate the functional roles of DYNLT3 during mouse oocyte meiosis, we employed antibody injection to examine its effect on chromosome alignment at the MI stage. We cultured the oocytes for 8 hours and then examined chromosome morphology by confocal microscopy. As shown in Figure 2A, the chromosomes were well-aligned in the control group oocytes (A1), while a large proportion of the oocytes displayed misaligned chromosomes in the antibody injection group (A2-4). Compared with the control group (27.0% $\pm$ 3.1%, n = 169; Figure 2B), the rate of chromosome misalignment was significantly higher in the antibody injection group (53.2% $\pm$ 4.8%, n = 168; $P < .05$).

We further proved that DYNLT3 depletion by antibody injection disrupts the attachments between microtubules and chromosomes. As shown in Figure 2C, after cold treatment oocytes were stained with CREST and α-tubulin. The results showed that the attachments were disrupted and the spindle fibers were scattered in the cytoplasm in the DYNLT3-depleted oocytes.

DYNLT3 Depletion Decreased Polar Body Extrusion (PBE) and Prevented Homologous Chromosome Segregation

To further dissect the roles of DYNLT3 during mouse oocyte meiotic maturation, we examined the effect of DYNLT3 on polar body extrusion (PBE). With 12 hours of culture, the
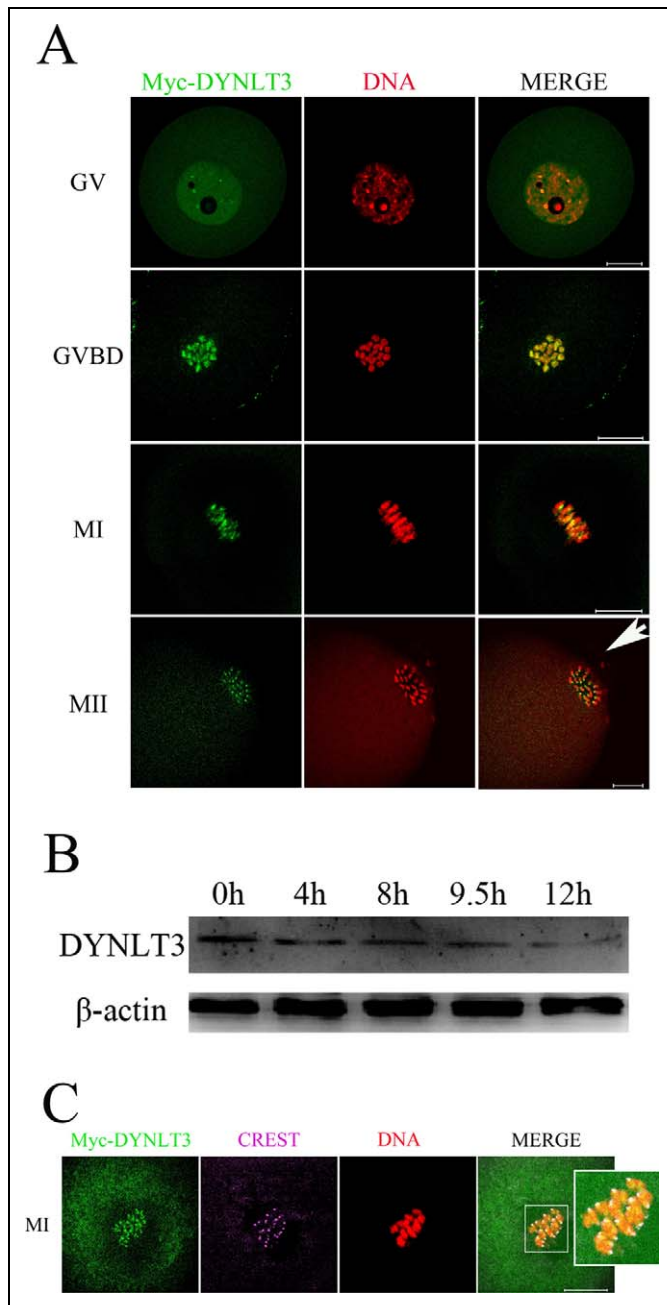
Figure 1. Localization and expression of DYNLT3 during mouse oocyte meiotic maturation. A, Localization of Myc-DYNLT3 revealed by immunofluorescent staining. In the germinal vesicle (GV) stage, Myc-DYNLT3 was mainly distributed in the GV. After germinal vesicle breakdown (GVBD), MI, and MII stages, Myc-DYNLT3 accumulated at the kinetochores of chromosomes. Green, Myc-DYNLT3; red, chromosomes. B, Expression of DYNLT3 was measured by Western blotting. Samples were collected after culture for 0, 4, 8, 9.5, and 12 hours, the time points when most oocytes reached the GV, Pro MI, MI, ATI, and MII stages, respectively. The molecular mass of DYNLT3 and β-actin were 13 kDa and 42 kDa, respectively. Each sample was collected from 280 oocytes. C, Colocalization of Myc-DYNLT3 with CREST at the kinetochores of metaphase chromosomes. Green, Myc-DYNLT3; purple, CREST; red, chromosomes. Arrows indicate first polar body. Bar = 20 μm.
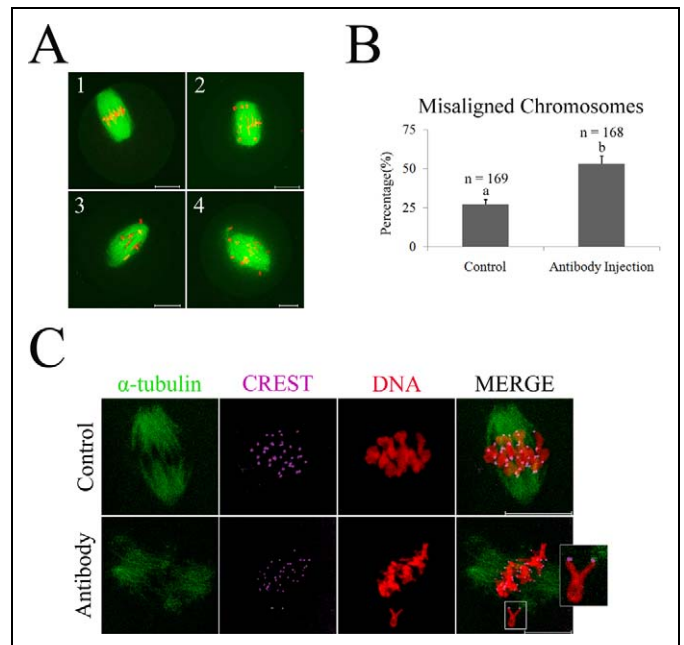

Figure 2. Effects of DYNLT3 depletion on homologous chromosome alignment and attachment of microtubules and chromosomes. A, MI spindle morphology and homologous chromosome alignment after microinjection of control immunoglobulin G (IgG) and DYNLT3 antibody in mouse oocytes. In the control IgG injection group, most oocytes showed normal chromosome alignment (A1), while in the antibody injection group, a large proportion of oocytes showed chromosome alignment disruption (A2-4). Green, α-tubulin; red, chromosomes. B, Rates of misaligned chromosomes in the control IgG and DYNLT3 antibody injection groups. Data are expressed as mean $\pm$ SEM of at least 3 repeated experiments and different letters indicate statistically significant difference ($P < .05$). C, Oocytes of the control IgG and DYNLT3 antibody injection group were cultured for 8 hours followed by cold treatment for 10 minutes in M2 medium which was precooled to 4°C. Then the oocytes were processed with immunostaining of α-tubulin and CREST. Magnification of the boxed region shows intact attachment between kinetochores and microtubules. Green, α-tubulin; purple, CREST; red, chromosomes. Bar = 20 μm.

majority of mouse oocytes normally extrude the first polar body (PB1) and enter the MII stage. So we cultured the oocytes for 12 hours and then examined the rate of PBE in both control and DYNLT3-depleted oocytes. As shown in Figure 3A, in the control group, most of the oocytes extruded PB1 ($78.3\% \pm 2.9\%$, n = 149); while in the DYNLT3 antibody injected group, the PBE rate was significantly lower ($56.5\% \pm 5.6\%$, n = 189; $P < .05$). Decrease of the PBE rate in DYNLT3 depleted oocytes indicated failure of metaphase I to anaphase I (MI-AI) transition.

To examine the details of homologous chromosomes during the delayed MI-AI transition, we further employed chromosome spread experiments. A typical bivalent shape displayed nondisjunctioned homologous chromosomes which were connected through arm regions. As shown in Figure 3B, after 12 hours of culture, the control antibody injected oocytes with PBE displayed normal 20 univalents sister chromatids.
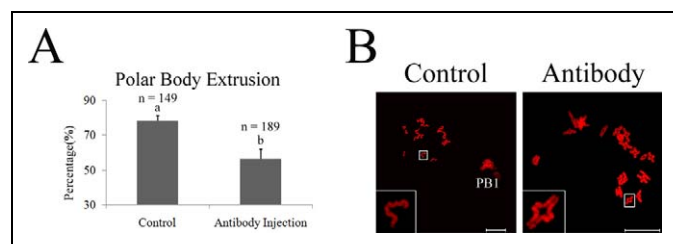
Figure 3. Effects of DYNLT3 depletion on meiotic cell cycle progression in mouse oocyte meiosis. A, Rates of polar body extrusion in the control immunoglobulin G (IgG) and DYNLT3 antibody injection groups after 12 hours of culture. Data are expressed as mean ± SEM of at least 3 repeated experiments and different letters indicate statistically significant difference (P < .05). B, Oocytes of control IgG and DYNLT3 antibody injection groups were cultured for 12 hours, followed by chromosome-spread experiments. Magnification of the boxed region shows segregated chromosomes (univalent) and unsegregated chromosomes (bivalent) in the control IgG and DYNLT3 antibody injection group, respectively. PB1 indicates first polar body. Bar = 20 μm.

However, in the DYNLT3 antibody-injected group, the oocytes whose MI-AI transition was inhibited displayed 20 bivalents, without any univalent. These results imply that depletion of DYNLT3 resulted in failure of MI-AI transion in mouse oocyte meiosis by preventing homologous chromosome segregation, but it did not cause aneuploidy.

Discussion

In this study, we have shown the localization, expression, and potential functions of DYNLT3 during mouse oocyte meiotic maturation. We demonstrated that dynein light chain DYNLT3 was required for chromosome alignment and meiotic maturation progression.

In mitosis, immunofluorescence microscopy studies with dynein antibodies demonstrated that dynein localized initially to kinetochores during prometaphase.[7] A later study reported that dynein light chain DYNLT3 was localized to kinetochores at prometaphase and spindle microtubules at metaphase in human mitosis.[38] DYNLT3 exhibited 86% sequence identity in mouse and human cells, which indicates that it may share some functions in mouse cells. In our study, we showed some similar results in oocyte meiosis. In the GV stage, DYNLT3 was restricted to the nucleus, and then concentrated at kinetochores in oocytes at GVBD, MI, and MII stages (Figure 1A). The distribution pattern of DYNLT3 at kinetochores was confirmed by colocalization of DYNLT3 and CREST (Figure 1C). Different from human mitosis, we did not detect any signal at spindle microtubules at MI, indicating that it may play a different role in meiotic metaphase. We inferred that DYNLT3 may play a potential role in kinetochore and microtubule attachment but not spindle assembly during oocyte meiosis.

We further blocked DYNLT3 function by antibody injection to analyze the effects of DYNLT3 on meiotic progression. Depletion of DYNLT3 caused severe chromosome misalignment at the MI stage (Figure 2A). Chromosomes had escaped from the spindle which indicated that microtubules may have lost attachments to kinetochores. We employed cold treatment and stained α-tubulin and CREST to examine the attachments between kinetochores and microtubules. Our results showed that DYNLT3 depletion caused detachment between kinetochores and microtubules, suggesting it could interact with microtubules (Figure 2C). It has been shown that dynein accumulates at kinetochores prior to microtubule attachment and is involved in the initial interactions with microtubules, which contributed to chromosome poleward movement.[8,9,12] The interaction of dynein with microtubules is well-established generally and in the early stages of mitosis.[43] When dynein is inhibited prior to microtubule attachment, congression defects and prometaphase arrest are observed.[44] In contrast, when dynein is inhibited during prometaphase, chromosomes approach the metaphase plate normally.[4] These results suggested that dynein plays a role in mitotic microtubule attachment. In addition, DYNLT3 is directly linked to SAC protein Bub3 in mitosis, suggesting that DYNLT3 together with Bub3 is involved in the formation of stable bipolar kinetochore attachments to microtubules.[38] In our study, DYNLT3 localized to kinetochores and depletion of DYNLT3 resulted in detachment of kinetochores and microtubules, suggesting that, as a component of dynein, DYNLT3 may interact with microtubules and may regulate dynein function in chromosome movement. Depletion of DYNLT3 disrupted kinetochore and microtubule attachments and may subsequently cause chromosome misalignment.

Furthermore, compared with the control IgG-injected oocytes, a lower proportion of DYNLT3 antibody-injected oocytes extruded PB1 after 12 hours of culture, indicating that oocytes failed to complete the normal meiosis progression in the DYNLT3 depletion group (Figure 3A). Chromosome-spread experiments further revealed that the homologous chromosomes failed to segregate and the oocytes were held at the MI stage (Figure 3B). Mouse oocytes were not able to progress through the MI stage until all chromosomes had established proper attachments to spindle microtubules and aligned at the metaphase plate.[45] The SAC was a surveillance mechanism that prevented chromosome mis-segregation by delaying the MI-AI transition. In our previous study, we found that SAC proteins, such as Bub3 and BubR1, localized to unattached kinetochores during prometaphase. Activation of SAC could result in failure of the MI-AI transition.[46,47] Once the last chromosome achieves proper bipolar attachment to the spindle, SAC is turned off, which is also known as SAC silencing. Mechanistically, the metaphase arrest phenotype reflects the inability of dynein to transport the anaphase inhibitor SAC away from kinetochores.[48] In this study, we have found that depletion of DYNLT3 caused detachment between microtubules and kinetochores. As a member of dynein light chain DYNLT family, DYNLT3 has been shown to link dynein to specific SAC Bub3 in human mitosis.[38] So we inferred that DYNLT3 deletion may result in failure of SAC transport from kinetochores, which led to MI arrest. However, further clarification is needed. The relationship between

DYNLT3 and SAC could be the next step to clarify DYNLT3 function in oocyte meiosis.

In conclusion, our data demonstrate that DYNLT3 localizes to kinetochores and participates in chromosome alignment by interacting with microtubules. Depletion of DYNLT3 impairs meiosis consistency and causes MI arrest, indicating its possible role in meiotic cell cycle progression.

Authors' Note

The authors Xin Huang and Hai-Long Wang contributed equally to this work.

Acknowledgement

Declaration of Conflicting Interests

The authors declared no conflicts of interest with respect to the authorship and/or publication of this article.

Funding

References

1. Yin S, Sun XF, Schatten H, Sun QY. Molecular insights into mechanisms regulating faithful chromosome separation in female meiosis. *Cell Cycle*. 2008;7(19):2997-3005.

2. Matsuura S, Ito E, Tauchi H, Komatsu K, Ikeuchi T, Kajii T. Chromosomal instability syndrome of total premature chromatid separation with mosaic variegated aneuploidy is defective in mitotic-spindle checkpoint. *Am J Hum Genet*. 2000;67(2):483-486.

3. Bader JR, Vaughan KT. Dynein at the kinetochore: timing, interactions and functions. *Semin Cell Dev Biol*. 2010;21(3):269-275.

4. Vaisberg EA, Koonce MP, McIntosh JR. Cytoplasmic dynein plays a role in mammalian mitotic spindle formation. *J Cell Biol*. 1993;123(4):849-858.

5. Busson S, Dujardin D, Moreau A, Dompierre J, De Mey JR. Dynein and dynactin are localized to astral microtubules and at cortical sites in mitotic epithelial cells. *Curr Biol*. 1998;8(9):541-544.

6. O'Connell CB, Wang YL. Mammalian spindle orientation and position respond to changes in cell shape in a dynein-dependent fashion. *Mol Biol Cell*. 2000;11(5):1765-1774.

7. Pfarr CM, Coue M, Grissom PM, Hays TS, Porter ME, McIntosh JR. Cytoplasmic dynein is localized to kinetochores during mitosis. *Nature*. 1990;345(6272):263-265.

8. Wordeman L, Steuer ER, Sheetz MP, Mitchison T. Chemical subdomains within the kinetochore domain of isolated CHO mitotic chromosomes. *J Cell Biol*. 1991;114(2):285-294.

9. Yang Z, Tulu US, Wadsworth P, Rieder CL. Kinetochore dynein is required for chromosome motion and congression independent of the spindle checkpoint. *Curr Biol*. 2007;17(11):973-980.

10. Wojcik E, Basto R, Serr M, Scaerou F, Karess R, Hays T. Kinetochore dynein: its dynamics and role in the transport of the Rough deal checkpoint protein. *Nat Cell Biol*. 2001;3(11):1001-1007.

11. Vorozhko VV, Emanuele MJ, Kallio MJ, Stukenberg PT, Gorbsky GJ. Multiple mechanisms of chromosome movement in vertebrate cells mediated through the Ndc80 complex and dynein/dynactin. *Chromosoma*. 2008;117(2):169-179.

12. Varma D, Monzo P, Stehman SA, Vallee RB. Direct role of dynein motor in stable kinetochore-microtubule attachment, orientation, and alignment. *J Cell Biol*. 2008;182(6):1045-1054.

13. Gee M, Vallee R. The role of the dynein stalk in cytoplasmic and flagellar motility. *Eur Biophys J*. 1998;27(5):466-473.

14. Oiwa K, Sakakibara H. Recent progress in dynein structure and mechanism. *Curr Opin Cell Biol*. 2005;17(1):98-103.

15. Vallee RB, Williams JC, Varma D, Barnhart LE. Dynein: an ancient motor protein involved in multiple modes of transport. *J Neurobiol*. 2004;58(2):189-200.

16. Habura A, Tikhonenko I, Chisholm RL, Koonce MP. Interaction mapping of a dynein heavy chain. Identification of dimerization and intermediate-chain binding domains. *J Biol Chem*. 1999;274(22):15447-15453.

17. Tynan SH, Gee MA, Vallee RB. Distinct but overlapping sites within the cytoplasmic dynein heavy chain for dimerization and for intermediate chain and light intermediate chain binding. *J Biol Chem*. 2000;275(42):32769-32774.

18. King SM, Barbarese E, Dillman JF, 3rd, et al. Cytoplasmic dynein contains a family of differentially expressed light chains. *Biochemistry*. 1998;37(43):15033-15041.

19. Lader E, Ha HS, O'Neill M, Artzt K, Bennett D. tctex-1: a candidate gene family for a mouse t complex sterility locus. *Cell*. 1989;58(5):969-979.

20. Caggese C, Moschetti R, Ragone G, Barsanti P, Caizzi R. dtctex-1, the Drosophila melanogaster homolog of a putative murine t-complex distorter encoding a dynein light chain, is required for production of functional sperm. *Mol Genet Genomics*. 2001;265(3):436-444.

21. Miki F, Okazaki K, Shimanuki M, Yamamoto A, Hiraoka Y, Niwa O. The 14-kDa dynein light chain-family protein Dlc1 is required for regular oscillatory nuclear movement and efficient recombination during meiotic prophase in fission yeast. *Mol Biol Cell*. 2002;13(3):930-946.

22. Dedesma C, Chuang JZ, Alfinito PD, Sung CH. Dynein light chain Tctex-1 identifies neural progenitors in adult brain. *J Comp Neurol*. 2006;496(6):773-786.

23. Tseng YY, Gruzdeva N, Li A, Chuang JZ, Sung CH. Identification of the Tctex-1 regulatory element that directs expression to neural stem/progenitor cells in developing and adult brain. *J Comp Neurol*. 2010;518(16):3327-3342.

24. Kai N, Mishina M, Yagi T. Molecular cloning of Fyn-associated molecules in the mouse central nervous system. *J Neurosci Res*. 1997;48(5):407-424.

25. Nagano F, Orita S, Sasaki T, et al. Interaction of Doc2 with tctex-1, a light chain of cytoplasmic dynein. Implication in dynein-dependent vesicle transport. *J Biol Chem*. 1998;273(46):30065-30068.

26. Bauch A, Campbell KS, Reth M. Interaction of the CD5 cytoplasmic domain with the Ca2+/calmodulin-dependent kinase IIdelta. *Eur J Immunol*. 1998;28(7):2167-2177.

27. Tai AW, Chuang JZ, Bode C, Wolfrum U, Sung CH. Rhodopsin's carboxy-terminal cytoplasmic tail acts as a membrane receptor for cytoplasmic dynein by binding to the dynein light chain Tctex-1. *Cell*. 1999;97(7):877-887.

28. Mok YK, Lo KW, Zhang M. Structure of Tctex-1 and its interaction with cytoplasmic dynein intermediate chain. *J Biol Chem*. 2001;276(17):14067-14074.

29. Nadano D, Nakayama J, Matsuzawa S, Sato TA, Matsuda T, Fukuda MN. Human tastin, a proline-rich cytoplasmic protein, associates with the microtubular cytoskeleton. *Biochem J*. 2002;364(pt 3):669-677.

30. Mueller S, Cao X, Welker R, Wimmer E. Interaction of the poliovirus receptor CD155 with the dynein light chain Tctex-1 and its implication for poliovirus pathogenesis. *J Biol Chem*. 2002;277(10):7897-7904.

31. Machado RD, Rudarakanchana N, Atkinson C, et al. Functional interaction between BMPR-II and Tctex-1, a light chain of Dynein, is isoform-specific and disrupted by mutations underlying primary pulmonary hypertension. *Hum Mol Genet*. 2003;12(24):3277-3286.

32. Sugai M, Saito M, Sukegawa I, et al. PTH/PTH-related protein receptor interacts directly with Tctex-1 through its COOH terminus. *Biochem Biophys Res Commun*. 2003;311(1):24-31.

33. Douglas MW, Diefenbach RJ, Homa FL, et al. Herpes simplex virus type 1 capsid protein VP26 interacts with dynein light chains RP3 and Tctex1 and plays a role in retrograde cellular transport. *J Biol Chem*. 2004;279(27):28522-28530.

34. Gauthier-Fisher A, Lin DC, Greeve M, Kaplan DR, Rottapel R, Miller FD. Lfc and Tctex-1 regulate the genesis of neurons from cortical precursor cells. *Nat Neurosci*. 2009;12(6):735-744.

35. Chuang JZ, Milner TA, Sung CH. Subunit heterogeneity of cytoplasmic dynein: Differential expression of 14 kDa dynein light chains in rat hippocampus. *J Neurosci*. 2001;21(15):5501-5512.

36. Wu H, Maciejewski MW, Takebe S, King SM. Solution structure of the Tctex1 dimer reveals a mechanism for dynein-cargo interactions. *Structure*. 2005;13(2):213-223.

37. Sachdev P, Menon S, Kastner DB, et al. G protein beta gamma subunit interaction with the dynein light-chain component Tctex-1 regulates neurite outgrowth. *EMBO J*. 2007;26(11): 2621-2632.

38. Lo KW, Kogoy JM, Pfister KK. The DYNLT3 light chain directly links cytoplasmic dynein to a spindle checkpoint protein, Bub3. *J Biol Chem*. 2007;282(15):11205-11212.

39. Apcarian A, Cunningham AL, Diefenbach RJ. Identification of binding domains in the herpes simplex virus type 1 small capsid protein pUL35 (VP26). *J Gen Virol*. 2010;91(pt 11):2659-2663.

40. Dohner K, Radtke K, Schmidt S, Sodeik B. Eclipse phase of herpes simplex virus type 1 infection: efficient dynein-mediated capsid transport without the small capsid protein VP26. *J Virol*. 2006;80(16):8211-8224.

41. Tai AW, Chuang JZ, Sung CH. Localization of Tctex-1, a cytoplasmic dynein light chain, to the Golgi apparatus and evidence for dynein complex heterogeneity. *J Biol Chem*. 1998;273(31): 19639-19649.

42. Yang S, Liu X, Yin Y, Fukuda MN, Zhou J. Tastin is required for bipolar spindle assembly and centrosome integrity during mitosis. *FASEB J*. 2008;22(6):1960-1972.

43. Paschal BM, Vallee RB. Retrograde transport by the microtubule-associated protein MAP 1C. *Nature*. 1987;330(6144):181-183.

44. Echeverri CJ, Paschal BM, Vaughan KT, Vallee RB. Molecular characterization of the 50-kD subunit of dynactin reveals function for the complex in chromosome alignment and spindle organization during mitosis. *J Cell Biol*. 1996;132(4):617-633.

45. Wassmann K, Niault T, Maro B. Metaphase I arrest upon activation of the Mad2-dependent spindle checkpoint in mouse oocytes. *Curr Biol*. 2003;13(18):1596-1608.

46. Li M, Li S, Yuan J, et al. Bub3 is a spindle assembly checkpoint protein regulating chromosome segregation during mouse oocyte meiosis. *PLoS One*. 2009;4(11):e7701.

47. Wei L, Liang XW, Zhang QH, et al. BubR1 is a spindle assembly checkpoint protein regulating meiotic cell cycle progression of mouse oocyte. *Cell Cycle*. 2010;9(6):1112-1121.

48. Zhang D, Yin S, Jiang MX, et al. Cytoplasmic dynein participates in meiotic checkpoint inactivation in mouse oocytes by transporting cytoplasmic mitotic arrest-deficient (Mad) proteins from kinetochores to spindle poles. *Reproduction*. 2007;133(4):685-695.